

# 1 Supplementary Information

## 2 1 Methods

### 3 1.1 Detailed explanation and evaluation on how hydrogel composition in aerosols was approximated

4 For the evaluation of abundances and size distribution of total hydrogels (including both Coomassie Stainable and  
5 Transparent Particles, CSP and TEP) in surface seawater (SSW) and sea spray aerosols (SSA), instructions of the  
6 classical Engel et al. (2009) methodology were implemented. The analysis of particles was conducted with the software  
7 *Image J*. Both, stained CSP and TEP particles appear blue (Fig. 2, main text). The images were split into the three  
8 RGB color stacks, representing the red, green, and blue channels. The red color channel was the least represented in  
9 the blue particles and thus selected for the analysis. It accentuates best the contrast of stained hydrogel particles in  
10 comparison to the white background of the filters. Using an *Image J* plug-in, the contrast of the particles is outlined  
11 and transformed into the equivalent spherical diameter (ESD) of individual particles.

12  
13 While for the precursors in SSW, two separate sets of filters were stained for CSP and TEP, respectively, only one  
14 filter per day was available to characterize SSA hydrogel composition. This filter was double-stained. Overall, the  
15 classical approach resulted in a complete data set for TEP and CSP in the SSW, comprising abundances and size  
16 distribution for each dye (classical approach), while the SSA data set was incomplete as it comprised only total  
17 abundances and size distributions, thereby including all double-stained particles irrespective of the dominating dye.  
18 To additionally separate the different blue tones and assess the approximate contribution of protein and carbohydrate-  
19 enriched hydrogels (CSP: dark blue, TEP: light blue, Fig. 2, main text), the three RGB channels of an image were  
20 converted into a HSL (hue, saturation, lightness) model of color, representing different tones ('hue') in a circular color  
21 scheme, which can be described in a single number (unit: degree; range: 0-360°). The resulting hue values and  
22 differences in intensity between the strongest and weakest pixels of RGB channels (chroma, ranging from 1 to -1) were  
23 used to define a specific range of colors representing TEP and CSP. The range was calibrated with artificial and natural  
24 particles derived from alginic acid (representative of TEP) or bovine serum albumin (representative of CSP) and  
25 seawater samples. Examples of the divergence in hue and chroma are showcased with natural samples and a blank in  
26 Fig. S1. An *Image J* plug-in was designed to evaluate each particle's color and therewith its identity (i.e., CSP or TEP).  
27 The approximate ratio of CSP to total SSA hydrogel abundance determined by using auxiliary hue values (CSP ratio  
28 in SSA\*) is represented in the top panel of Fig. 5 in the main text and in Table 1, separated by size bins. The ratio of  
29 CSP area of hydrogels in SSA is further presented in Table A4 (main text).

30  
31 Applying different staining and evaluation approaches to assess the CSP ratio of hydrogels in SSW and SSA entails  
32 certain caveats. While the classical method has been established for nearly three decades (A. Long & Azam, 1996) and  
33 widely applied for over two decades (Engel, 2009), the modified approach presented here has so far been tested on a  
34 limited sample set and was calibrated using model substances. Consequently, the results should be interpreted with  
35 caution and regarded as an approximation of the true hydrogel composition in SSA.

36 Nevertheless, several independent lines of evidence support the validity and robustness of the modified approach.  
37 Across eight samples representing four distinct biogeochemical regimes, the SSA CSP ratio in abundance differed by  
38  $37.5 \pm 12\%$  (mean  $\pm$  SD), while the ratio based on SSA particle area differed by  $9.4 \pm 4.4\%$ , indicating consistent  
39 compositional patterns despite environmental variability. The HSL conversion-based analysis indicates that hydrogels  
40 in SSA are dominated by carbohydrate-like material, a finding that is consistent with the correlation matrix (Fig. 6b),  
41 which shows that hydrogel abundance in SSA is most strongly associated with TEP occurrence in the SSW.  
42 Importantly, the size-binned hydrogel abundances in SSA and SSW shown in Fig. 6b are independent of the HSL  
43 conversion and rely solely on the red channel (RGB) selection criteria as used by the classical approach. Furthermore,  
44 the interpretation of compositional differences across SSA size bins (CSP ratio in SSA\*) is consistent with previously  
45 published findings (Jayarathne et al., 2016; Triesch et al., 2021; Wang et al., 2015).

46 Taken together, the consistency across contrasting regimes, the agreement between the modified approach, the classical  
47 RGB-based evaluation, and existing literature provides sufficient confidence to include the approximated CSP ratio of  
48 hydrogels in SSA into our results and interpretation.

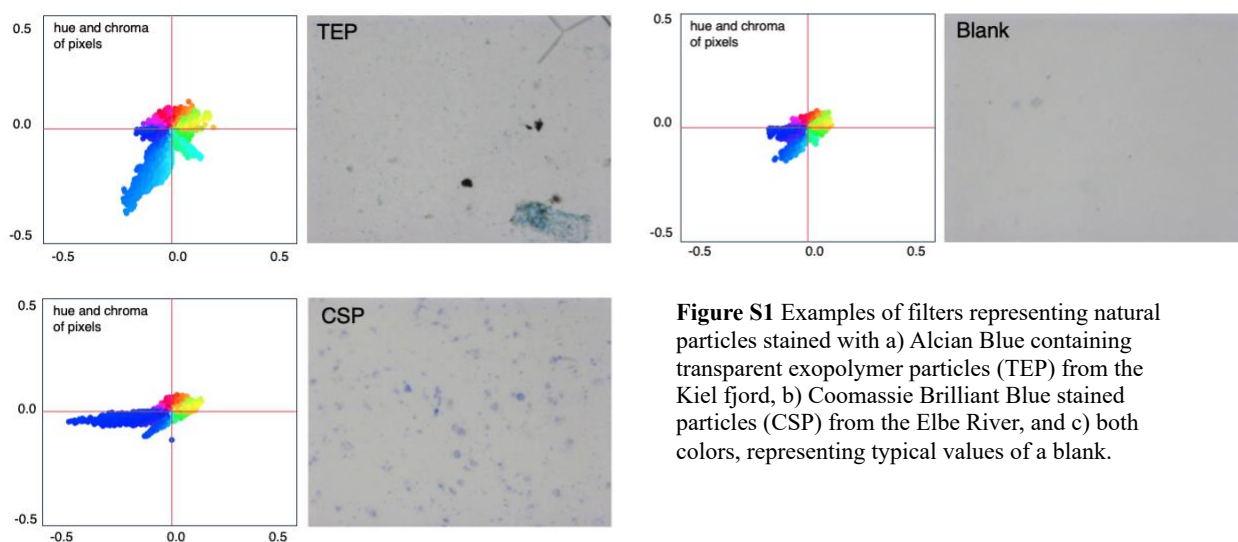


**Figure S1** Examples of filters representing natural particles stained with a) Alcian Blue containing transparent exopolymer particles (TEP) from the Kiel fjord, b) Coomassie Brilliant Blue stained particles (CSP) from the Elbe River, and c) both colors, representing typical values of a blank.

49

## 50 References

- 51 Engel, A. (2009). *Determination of Marine Gel Particles, Practical guidelines for the analysis of seawater* (O.  
52 Wurl, B. Raton, & [u.a.] (eds.)). CRC Press.
- 53 Long, R. A., & Azam, F. (1996). Abundant protein-containing particles in the sea. *Aquatic Microbial Ecology*, *10*(3),  
54 213–221. <https://doi.org/10.3354/ame010213>.
- 55 Jayarathne, T., Sultana, C. M., Lee, C., Malfatti, F., Cox, J. L., Pendergraft, M. A., Moore, K. A., Azam, F.,  
56 Tivanski, A. V., Cappa, C. D., Bertram, T. H., Grassian, V. H., Prather, K. A., & Stone, E. A. (2016). Enrichment of  
57 Saccharides and Divalent Cations in Sea Spray Aerosol during Two Phytoplankton Blooms. *Environmental Science*  
58 *and Technology*, *50*(21), 11511–11520. <https://doi.org/10.1021/acs.est.6b02988>.

59 Triesch, N., Van Pinxteren, M., Engel, A., & Herrmann, H. (2021). Concerted measurements of free amino acids at  
60 the Cabo Verde islands: High enrichments in submicron sea spray aerosol particles and cloud droplets. *Atmospheric*  
61 *Chemistry and Physics*, 21(1), 163–181. <https://doi.org/10.5194/acp-21-163-2021>.  
62 Wang, X., Sultana, C. M., Trueblood, J., Hill, T. C. J., Malfatti, F., Lee, C., Laskina, O., Moore, K. A., Beall, C. M.,  
63 McCluskey, C. S., Cornwell, G. C., Zhou, Y., Cox, J. L., Pendergraft, M. A., Santander, M. V., Bertram, T. H.,  
64 Cappa, C. D., Azam, F., DeMott, P. J., ... Prather, K. A. (2015). Microbial control of sea spray aerosol composition:  
65 A tale of two blooms. *ACS Central Science*, 1(3), 124–131. <https://doi.org/10.1021/acscentsci.5b00148>.